Directional Solidification: Transition from Cells to Dendrites

Y. Saito,[a] C. Misbah,[b] and H. Müller-Krumbhaar
Institut für Festkörperforschung der Kernforschungsanlage Jülich, D-5170 Jülich, West Germany
(Received 14 August 1989)

The evolution of cells and dendrites on a solidification front is analyzed numerically by a Green's-function method. We obtain a consistent picture of the pattern-forming processes in the whole experimentally accessible range of the phase diagram of *cell spacing* versus *growth rate*. We find a smooth transition from cells to free dendrites confirming suspected scaling relations. The selection of dendritic spacings appears to occur through a *tail instability*.

PACS numbers: 61.50.Cj, 05.70.Fh, 68.70.+w, 81.30.Fb

The solidification of most alloys occurs under conditions known as *directional solidification*.[1,2] The solid-liquid interface is forced by a wandering thermal field into the liquid, thereby segregating impurities in a thin layer in front of the interface. At sufficiently high speeds $v > v_c$ this layer becomes effectively supersaturated and the originally flat interface becomes wrinkled,[2] then cellular, and finally an array of parallel growing dendrites is formed. Even though the mathematical (Stefan) problem was formulated a long time ago[2] most of the interesting questions still are unanswered: What is the spacing of the primary cells or dendrites, is there a discontinuous transition between them, how important are the grooves between the cells, and what is the role of crystalline anisotropy?

For experimental investigations[3-6] one typically uses a flat vessel made of two thin glass plates which is moved in a temperature field with a constant thermal gradient along the growth direction. This should approximate two-dimensional growth phenomena, but at high growth rates the patterns usually become finer than the gap between the glass plates. Material parameters such as surface tension, anisotropy, segregation, and diffusion coefficients are only known with appreciable uncertainties, such that, for example, the instability of an initially flat front can only be matched with an error of about (20–50)% relative to theoretical predictions.

Analytical calculations[7,8] which were successful in free dendritic growth[9,10] are still subject to discussion concerning, for example, the boundary conditions deep in the grooves or the range of Peclet numbers typical for experiments. Numerical calculations[11] so far have been performed on stationary patterns only, not exploring the dendritic region. As we have also found, the stationary calculations sometimes give solutions which are unreachable dynamically.

Since both the experimental and the theoretical results leave a wealth of open questions and do not seem to agree very well with each other, we have made a systematic investigation by a time-dependent numerical Green's-function code[10] based on the quasistationary approximation. This approximation still correctly identifies the occurrence of instabilities of a stationary growing pattern if the bifurcation is not of Hopf type.

The well-known model[1,2,11] is defined as follows:

$$\frac{1}{D}\frac{\partial}{\partial t}u(x,z,t) \approx 0 = \nabla^2 u + \frac{2}{l}\frac{\partial}{\partial z}u\,, \tag{1}$$

$$u_l = 1 - d(\theta)K - \zeta(x,t)/l_T\,, \tag{2}$$

$$-(D_l \hat{\mathbf{n}}\cdot\nabla u_l - D_s \hat{\mathbf{n}}\cdot\nabla u_s) = [1+(1-k)(u_l-1)]v_n\,. \tag{3}$$

Equation (1) is the diffusion equation in quasistationary approximation in a frame of reference moving at velocity v in the z direction, $l = 2D/v$ is the diffusion length, and D is the diffusion constant. u is the normalized field of impurity concentrations. Equation (2) is the boundary condition for the diffusion field v_l at the interface; at infinity one has $u = 0$. Note that $u_l = 1$ is a necessary condition for a flat interface growing at constant speed. $d(\theta) = d_0[1 - \epsilon\cos(4\theta)]$ is the anisotropic capillary length, K is the curvature, ζ is the relative displacement of the interface from a plane front moving at constant speed, and l_T is the thermal length as a measure of the (inverse) thermal gradient prescribed by the experimental setup. Equation (3) is the conservation law for the solute or impurity at the interface; D_l and D_s are the diffusion coefficients in the liquid and solid, u_l and u_s are the concentrations at the interface in the liquid and solid, and v_n is the velocity of the interface in the normal direction $\hat{\mathbf{n}}$. The segregation coefficient $0 \le k$ influences the type of bifurcation of the initially flat interface into a corrugated structure: For small k the bifurcation is inverted; for $k \approx 1$ it is normal. Both situations are encountered in typical experiments.

The numerical parameters of the model were representatively taken to correspond to *steel* with Cr and Ni ingredients, and in dimensionless units are $l_T = 1$, $D_l = 1$, $D_s = 0$, $k = 0.9$, and $d_0 = 2.95 \times 10^{-4}$, the critical velocity and wavelength for the plane-front instability resulting as $v_c = 1.136$, $\lambda_c = 0.514$. The anisotropy of the capillary length is unknown and was taken as $\epsilon = 0.1$ to allow for comparison with our previous calculations on the free dendritic case. A sinusoidal perturbation (with mirror boundary conditions) was chosen as the starting condi-

tion. Further details, concerning, for example, the competition of several cells, will be given elsewhere.

The numerical code discretizes the interface by linear segments about $\frac{1}{5}$ of the tip radius in length. The time step is automatically adjusted to keep instantaneous changes of local curve characteristics below 0.1. Computing time for one parameter set until convergence varied between 10 min and 20 h on a Cray XMP, from low to high growth rates and anisotropies.

The program reproduces the neutral stability curve (Fig. 1) of a linear stability analysis[2] by better than 2%, for cases of normal and inverse bifurcation and for different ratios D_s/D_l. In Fig. 1 we show the phase diagram plotted here as $\log_{10}$(velocity) versus $\log_{10}$(wavelength). In principle, v is the experimentally prescribed quantity, but we plot it here on the y axis to emphasize similarities and differences with hydrodynamic pattern formation like in Rayleigh-Bénard systems. In that sense our pulling rate v corresponds to the Rayleigh number there. Not shown is the region of very large v, where the neutral stability curve closes again, in contrast to the hydrodynamic case. That region, however, is not easily accessible experimentally and hence will not be discussed here. The asterisks in Fig. 1 mark the series of numerical experiments presented in the following.

In a very small region above the lower limit of stability sinusoidal structures are formed. Keeping the wavelength at $\lambda=0.36$ and increasing the pulling rate to $v=4.0,7.65$ fingerlike elongated cells are formed as found similarly by other authors[11] before. The patterns do not yet resemble the parabolic and sidebranching structures of dendrites.

At velocities $v=12$ and higher the fingers become more and more parabolic at the tip while simultaneously sidebranches appear in the grooves between the fingers.

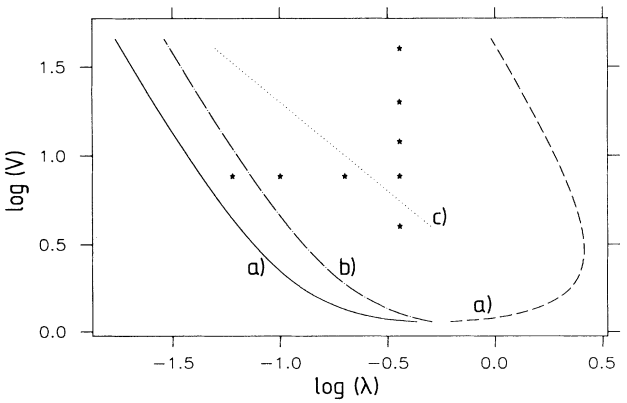

FIG. 1. Phase diagram of *velocity vs wavelength* in $\log_{10}$-$\log_{10}$ representation. Curve *a* is the curve of neutral stability of a plane front, curve *b* is the location of the most rapidly growing mode, and along curve *c* the wavelength equals the diffusion length. The asterisks mark the parameters of the simulations discussed here.

In Fig. 2, lower part, we show three snapshots of a sidebranching structure moving from left to right. The leftmost corresponds to a stationary sidebranching dendritic cell, moving at velocity $v=20$. Note that the fixed primary wavelength $\lambda=0.36$ is a factor of 14 larger than the wavelength at the left branch of the neutral stability curve in Fig. 1. Even larger ratios can be obtained at larger values of the anisotropy ϵ. Thus, a splitting of the primary spacing by a factor from 2 to 10 would still have rendered structures safely inside the neutral curve. A sudden increase of the pulling rate to $v=40$ gives the evolution shown in Fig. 2. The third sidebranch from the tip begins to grow out so far into the grooves as to become a new primary branch. The original dendrite maintains its identity; i.e., this is not a tip-splitting process, but rather a *tail instability*. This observation is quite in agreement with experiments,[4-6] where the adjustment of dendritic spacings does not seem to occur by a phase diffusion of the primary branches but by this uprise of a new cell out of a sidebranch in the groove. Hereby the spacing is reduced locally by a factor of 2; in our simulation it is a factor of 3 because of imposed mirror symmetry. This tail instability seems to depend sensitively on the anisotropy ϵ: For $\epsilon=0.05$ the instability becomes so strong that it leads to a splitting of the tip, while at $\epsilon=0.2$ the primary dendrites remain stable over displacements of more than ten spacings λ. If, as it now looks, the wavelength selection in the dendritic region occurs through this instability of a sidebranch, it will be a rather difficult problem to handle analytically.

Note that the diffusion length at these velocities is smaller than the spacing between the individual den-

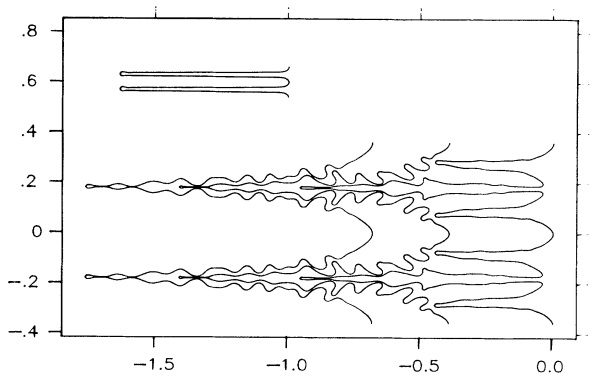

FIG. 2. Lower part: Three stroboscopic plots of a sidebranching structure moving from left to right, with solid on the left and liquid on the right. The leftmost dendrite running at velocity $v=20$ has reached a stationary sidebranching state. Then v was suddenly increased to 40. The following two plots show the evolution of the tail instability such that a new primary cell (plus its mirror image) is formed out of a sidebranch. Upper part: Short-wavelength limit of a cell at $v=7.65$ forming relatively wide grooves in accordance with the Saffman-Taylor scaling (axes in units of l_T).

drites. As the tips of the cells interact with each other through the diffusion field, this interaction has become exponentially weak. One therefore expects that the previously confirmed scaling relations for free dendrites[10] should hold just as well in the present case. This is demonstrated in Fig. 3. There we compare the actually measured tip radius with the radius R_s obtained from the scaling relation $2D_l d_0/vR_s^2=\text{const}(\epsilon)$ [Fig. 9 and Eq. (41) of Ref. 10] and alternatively with the Ivantsov radius $R_{\text{Iv}}=pl$, where the Peclet number p is taken as a measure of the supersaturation,

$$u_l(\text{tip})=\Delta=(\pi p)^{1/2}e^p\text{erfc}(\sqrt{p})\,.$$

This latter relation comes from the solution of the diffusion equation [(1)–(3)] around a parabolic boundary with tip radius R_{Iv} and represents basically a global conservation law for an isolated parabolic cell. Apparently this ceases to be applicable at velocities close to the threshold v_c where several cells compete for the same diffusion field. On the other hand, the scaling relation $R=R_s$ seems to be very robust as it already holds (with an error of about 10% due to numerical fluctuations) for velocities as low as $v=4$. We also checked that the wavelength of the sidebranches scales like the stability length $2\pi(ld_0)^{1/2}$ with a prefactor of about 2.5 independent of ϵ as in the case of free dendritic growth (Fig. 10 of Ref. 10). This holds as soon as sidebranches become visible.

The other interesting limit is the region of small cell spacings λ such that the diffusion length becomes much larger than λ. This should be analogous to the Saffman-Taylor viscous fingering[7] in a channel. A result is shown in Fig. 2, the small pattern in the upper part of the figure, with scale identical to the dendritic case. The cell spacing is now $\lambda=0.06$ corresponding to the leftmost asterisk of Fig. 1 at $v=7.65$. The pattern is significantly different from patterns at larger spacings as the grooves between the fingers are now rather wide. Measuring the width of the finger λ_f at about one wavelength behind the tip one recovers the predicted Saffman-Taylor scaling[7] ($\lambda_f=\Delta\lambda$, etc.) within a few percent. Of course the diffusion length and the thermal length are not really infinite so that the grooves become narrower towards the bottom.

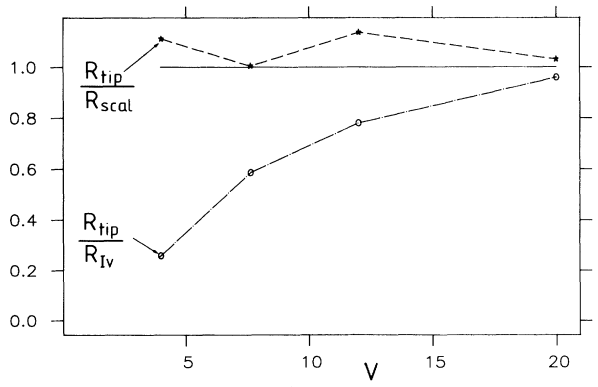

FIG. 3. Ratios of actual tip radius over Ivantsov radius (circles) and over the radius predicted from free dendritic scaling (Ref. 10) (asterisks) plotted vs growth rate.

In summary, we have identified a typical scenario for pattern formation in directional solidification consistent with various scaling assumptions. The interface forms dendritic patterns if both the diffusion length and the tip radius calculated from the free dendrite scaling[10] become smaller than the spacing λ of the cells. The transition from cells at low velocities to dendrites at high velocities is a very gradual process. So far we have found no indication for an oscillatory instability[8] during this transition which, however, may be suppressed by our quasistationary approximation. Furthermore, we have no explanation for the change in wavelengths reported[5,6] from experiments for this transition. Note, however, that in these experiments there occurs a transition from two- to three-dimensional cells as the tip radii become smaller than the gap between the glass plates. This happens typically in the same parameter range.[4]

These dendritic patterns fulfill the scaling relations for free dendrites including the sidebranching wavelength. The dendrites can apparently maintain large spacings at high velocities, as they operate as almost independent structures. This is in agreement with recent experiments.[3] A reduction of these spacings seems to occur typically through a tail instability such that a sidebranch serves as the origin of a new primary dendrite.

At small velocities and short wavelengths such that the diffusion length becomes much larger than the wavelength or spacing of the cells one reaches a limit, where the cells are separated by wide grooves and the tip radius scales with the width. This is in quantitative agreement with the analytical results for the Saffman-Taylor problem.[7]

Since it is not obvious how to perform conclusive experiments for questions such as what happens in the limit of $\epsilon\rightarrow 0$, and what controls the tail instability, we hope to report on numerical simulations on some of these aspects in the near future.

We thank S. de Cheveigne, C. Guthmann, P. Kurowski, G. Lesoult, and W. Kurz for giving us their experimental data prior to publication.

[a]Permanent address: Physics Department, Keio University, Yokohama, Japan.

[b]Permanent address: Groupe de Physique de Solides, Université de Paris VII, place Jussieu, 75251 Paris, France.

[1]J. S. Langer, Rev. Mod. Phys. **52**, 1 (1980).

[2]W. W. Mullins and R. F. Sekerka, J. Appl. Phys. **35**, 444 (1964); D. J. Wollkind and L. A. Segel, Philos. Trans. Roy.

Soc. London **51**, 268 (1970); B. Caroli, C. Caroli, and B. Roulet, J. Phys. (Paris) **43**, 1767 (1982).

[3]J. Bechhoefer and A. Libchaber, Phys. Rev. Lett. **35**, 1393 (1987).

[4]S. de Cheveigne, C. Guthmann, and M. M. Lebrun, J. Phys. (Paris) **47**, 2095 (1986).

[5]V. Seetharamen, M. A. Eshelmann, and R. Trivedi, Acta Metall. **36**, 1175 (1988).

[6]H. Esaka and W. Kurz, J. Cryst. Growth **72**, 578 (1985); W. Kurz and D. J. Fisher, in *Solidification* (Trans. Tech., Aedermannsdorf, 1984).

[7]P. Pelce and A. Pumir, J. Cryst. Growth **73**, 337 (1985); D. A. Kessler, J. Koplik, and H. Levine, Phys. Rev. A **34**, 4980 (1986); E. A. Brener, M. B. Geilikman, and D. E. Temkin, Zh. Eksp. Teor. Fiz. **94**, 241 (1988) [Sov. Phys. JETP **67**, 1002 (1988)]; (to be published).

[8]A. Karma and P. Pelce, Phys. Rev. A **39**, 4162 (1989).

[9]For recent reviews, see J. S. Langer, in *Proceedings of the Les Houches Summer School, Session 46,* edited by J. Souletie, J. Vanimenus, and R. Stora (Elsevier, Amsterdam, 1987); D. Kessler, J. Koplik, and H. Levine, Adv. Phys. **37**, 255 (1988).

[10]Y. Saito, G. Goldbeck-Wood, and H. Müller-Krumbhaar, Phys. Rev. A **38**, 2148 (1988), and references therein.

[11]L. H. Ungar and R. A. Brown, Phys. Rev. B **31** 5931 (1985); N. Ramprasad, M. J. Bennett, and R. A. Brown, Phys. Rev. B **38**, 583 (1988); D. Kessler and H. Levine, Phys. Rev. A **39**, 3041 (1989).